LA-3755

80

LOS ALAMOS SCIENTIFIC LABORATORY
of the
University of California
LOS ALAMOS • NEW MEXICO

The 1965 ARPA-AEC Joint Lightning Study at Los Alamos

Volume II

UNITED STATES
ATOMIC ENERGY COMMISSION
CONTRACT W-7405-ENG. 36

18

This report expresses the opinions of the author or authors and does not necessarily reflect the opinions or views of the Los Alamos Scientific Laboratory.

Printed in the United States of America. Available from Clearinghouse for Federal Scientific and Technical Information National Bureau of Standards, U. S. Department of Commerce Springfield, Virginia 22151

Price: Printed Copy $3.00; Microfiche $0.65

LA-3755
UC-34, PHYSICS
TID-4500

LOS ALAMOS SCIENTIFIC LABORATORY
of the
University of California
LOS ALAMOS • NEW MEXICO

Report written: July 1967

Report distributed: February 9, 1968

The 1965 ARPA-AEC Joint Lightning Study at Los Alamos*

Volume II

The Lightning Spectrum as Measured by Collimated Detectors. Atmospheric Transmission. Spectral Intensity Radiated.

by

Guy E. Barasch

*Work done under the auspices of the AEC in response to ARPA Order No. 631, Program Code No. 5820.

THE 1965 ARPA-AEC JOINT LIGHTNING STUDY AT LOS ALAMOS

VOLUME II

THE LIGHTNING SPECTRUM AS MEASURED BY COLLIMATED DETECTORS. ATMOSPHERIC TRANSMISSION. SPECTRAL INTENSITY RADIATED.

Guy E. Barasch

ABSTRACT

Collimated 50°-field photometers were operated during the 1965 lightning study to obtain data for an analysis of the production of false alarms in air-fluorescence nuclear-explosion detection systems. Detectors were employed in spectral regions useful for air-fluorescence detection: 3914 Å [N_2^+ 1N (0,0)] and 8900 Å [N_2 1P (1,0)], both of which are continuum channels for lightning; and at wavelengths useful for lightning discrimination: 4140 Å [continuum], 6563 Å [Hα], and 8220 Å [NI (2)]. Results from ~ 870 pulses in 58 flashes, all of which had visible, discrete channels, are presented in terms of source spectral intensities at 3914 Å (W sr^{-1} $Å^{-1}$) and as ratios of the spectral intensities in other wavelength regions to that at 3914 Å. Distances to the channels, ranging from 3 to 80 km, were measured using a photographic triangulation system, and appropriate inverse-square-law and atmospheric-transmission corrections were made.

Observations were made on all types of lightning phenomena: leaders, return strokes, and inter- and intra-cloud processes. The most probable spectral intensity at 3914 Å for all these pulses is 10^4 W sr^{-1} $Å^{-1}$; values range from 3×10^2 to 10^7 W sr^{-1} $Å^{-1}$. Average spectral intensities relative to 3914 Å are: 4140 Å, 1.2 ± 0.5; 6563 Å, 2.1 ± 0.8; 8220 Å, 4.8 ± 2.8; and 8900 Å, 0.8 ± 0.4. In first return strokes, the three longest-wavelength signals decrease relative to the 3914-Å signal by a factor of 1.5 to 3.

I. INTRODUCTION

This is the second of two reports on the optical emission characteristics of lightning, investigated at Los Alamos during the summer of 1965. Because lightning pulses are capable of producing false alarms in nuclear-explosion-detection systems that rely on optical detection of the burst of air fluorescence excited directly or indirectly by an explosion, a lightning study was conducted to find optimum methods to discriminate against such false

alarms. A number of types of optical detectors were operated with strict timing coordination to obtain different kinds of spectral information. Collimated photometers obtained time-resolved signals which were recorded continuously by oscilloscope cameras; results are reported here. A slitless spectrograph was used to investigate the return-stroke spectrum, for which results are given by Connor[1] in the first report of this series. All-sky photometers, identical to the ones designed for the Los Alamos Air Fluorescence Detection System (LAAFDS),[2] were operated by EG&G to measure the lightning spectrum as seen by the LAAFDS; preliminary results were reported by Amato.[3] All measurements have been reduced by inverse-square-law and atmospheric-transmission corrections to give source characteristics, using source-to-detector distances measured with a photographic triangulation system. Remotely operated, time-coordinated cameras recorded images of the optical channel of a lightning flash simultaneously from three separated stations.* Parallax measured from pairs of photographs of each channel, together with measurements of known landmarks, was used to calculate the slant distances to points on the channels. An average projected baseline of 650 m between pairs of stations resulted in estimated errors of ± 5% at a distance of 20 km and ± 25% at 80 km.*

Krider has reported photoelectric measurements of lightning made with collimated detectors, with both narrow spectral passbands[4] and broadband.[5] He was interested in the times at which radiation from the various molecular and atomic species reached its peak,[4] and in the advance rate of the return-stroke streamers;[5] he gave no relative strengths of the detected signals as a function of wavelength.

Subsequent reports will contain the applications of the results of the optical-emission measurements reported here and elsewhere.[1,3] Volume III will contain a derivation of the propagation characteristics of lightning-produced signals by which light is scattered into an all-sky detector. An aggregate of collimated-detector relative and absolute spectral data is required for comparison with similar all-sky detector results to obtain the scattering parameters. Volume IV will treat discrimination against lightning by nuclear-explosion air-fluorescence detection systems, and requires the distribution functions of source characteristics presented in this report.

II. INSTRUMENTATION AND CALIBRATION

Five "collimated" photometers with parallel, circular, 50° fields of view were used during each lightning storm. The term "collimated" is derived from the collimation of light by lenses before it passes through interference filters. The center of the common field of view was approximately parallel to that of the slitless spectrograph[1] at all times. In use, the spectrograph and photometers were pointed toward the greatest lightning activity; hence, for ~ 60% of the recorded flashes, the actual lightning source and the majority of the light scattered from it by clouds were within the photometers' field of view.

A. Instrumentation

A block diagram of a typical collimated-photometer recording channel is shown in Fig. 1. Signals from the photometer were amplified, conducted to the recording station, displayed on oscilloscopes, and recorded on 35-mm film. Logarithmic-response

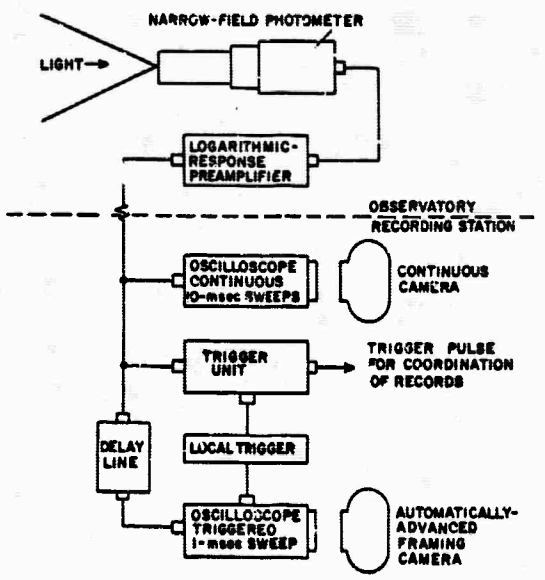

Fig. 1. Typical collimated-photometer recording channel. The observatory and recording station were 150 ft apart.

* Operated by EG&G, Inc.; data analyzed by LASL.

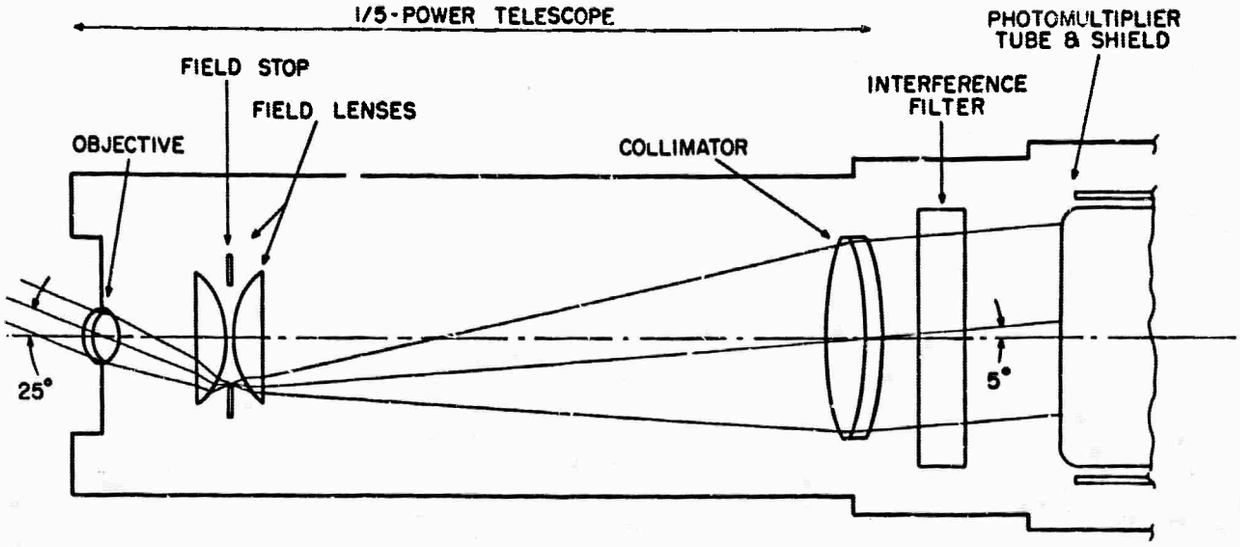

Fig. 2. Collimated-photometer optics. The telescope limits incidence angles of light rays at the interference filter.

amplifiers were used to permit the compression of several decades of useful data onto each recording; two oscilloscope beams were used for each photometer output as shown in Fig. 1.

The optical components of the photometer are shown in Fig. 2. Collimation of the incident light, and definition of the field of view, are accomplished by the four lenses and aperture, which form a telescope with a demagnification of 5. Light rays incident on the objective lens at angles $\leq 25^{\circ}$ off-axis leave the collimating lens and pass through the interference filter at angles $\leq 5^{\circ}$ from the normal. This collimation serves to limit both the wavelength shift and broadening of the spectral passband to less than 5 Å.

Interference-filter peak wavelengths are given in Table I. The average shift of the photometer passband from the filter passband due to oblique rays is -3 Å and thus is a small fraction of the bandwidth. Appropriate blocking filters were used.

The logarithmic-response amplifiers used Philbrick, Inc., operational-amplifier modules. The

Table I. Interference Filters Used in the Collimated Photometers.

Channel Wavelength (Å)	Filter-peak Wavelength (Å)	Bandwidth Half Max (Å)	Maximum Transmittance	Spectral Feature	Stronger Excitation in:
3914	3918	23	0.30	N_2^+ 1N(0,0)	Air Fluorescence
4140	4142	18	0.40	NI (6)	Lightning
6563	6565	16	0.64	H_α	Lightning
8220	8220	72	0.71	NI (2)	Lightning
8900	8900	65	0.55	N_2 1P(1,0)	Air Fluorescence

output, E (V), to a current pulse, I (A), was, to a good approximation,

$$E = E_o \log_{10} \left(\frac{I}{I_b} + 1 \right) ,$$

where E_o is a constant and I_b is the direct current flowing before the pulse. The actual output, E, as a function of I/I_b for one of the amplifiers used is shown in Fig. 3.

Continuous recordings of the output of each photometer were made on moving film using a "raster" display of recurrent 10-msec oscilloscope sweeps. This technique has been used by previous investigators of lightning[6] in order to record with relatively good resolution throughout the total duration of a lightning flash, which can be > 1.5 sec. Signals from two channels, adjusted to deflect in opposite directions, were recorded simultaneously by each dual-beam-oscilloscope camera. A typical pair of continuously recorded lightning signals is shown in Fig. 4.

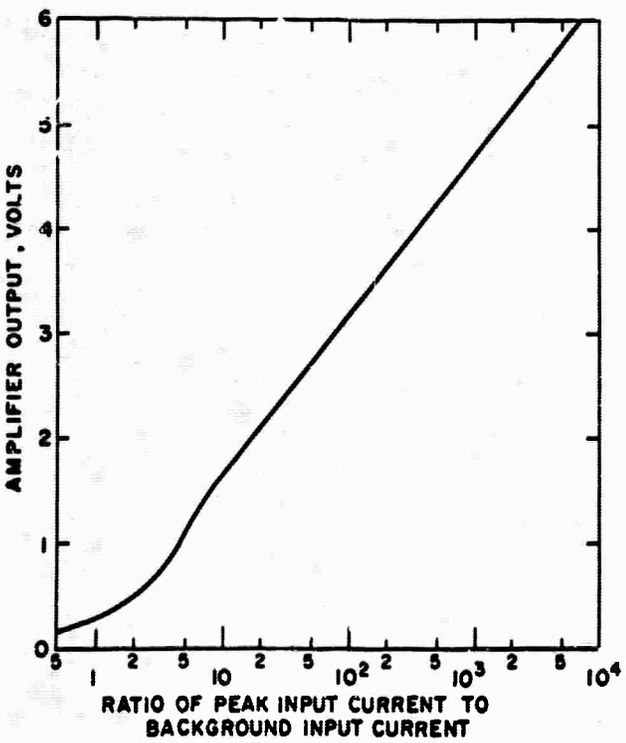

Fig. 3. Typical logarithmic-amplifier response curve. The input must be expressed as a ratio because of the logarithmic behavior.

The output signal from each collimated-detector channel was also recorded on a 1-msec-duration single sweep that was triggered by a "coordinated-trigger pulse," provided simultaneously to all the recording stations by the collimated detectors. The coordinated-trigger pulse was used at all recording stations to impress time marks by which simultaneous records could subsequently be correlated. Only a few of the collimated-photometer, single sweep recordings have been reduced; they will be reported elsewhere.

B. Photometer Calibrations

Absolute calibration of each of the photometers was performed by W. Gould immediately after the 1965 operation. Three sets of measurements were made for each photometer.

1. A tungsten primary-standard lamp which produced a known spectral irradiance at a given distance was used in conjunction with a mechanical shutter, operated at 1/500 sec, to obtain one point on a curve of spectral sensitivity, $S_V(\lambda_o)$, vs multiplier voltage, V, for each photometer. The value of the spectral irradiance, $H_c(\lambda_o)$ (W cm^{-2} Å^{-1}), at the peak transmission wavelength, λ_o, of the interference filter, was used to calculate the average sensitivity, $S_V(\lambda_o)$ [A/(W cm^{-2} Å^{-1})], as follows:

$$S_V(\lambda_o) = I_c \, H_c(\lambda_o) ,$$

where I_c is the current produced by the calibration pulse.

2. Relative sensitivities, $S_V(\lambda_o)$, defined above, were determined for all the operating voltages, V, by using a xenon-flash continuum source. They were related to the one absolute-response measurement made using the shuttered-tungsten source, giving a series of absolute pulse sensitivities for the multiplier voltages used.

3. A fatigue effect was found in several of the photometers at high background-light levels that depressed the sensitivities below their zero-background values. The factors by which the sensitivities were depressed were measured as a function of dc photometer output using the apparatus shown in Fig. 5. A uniform background over the 50° field of

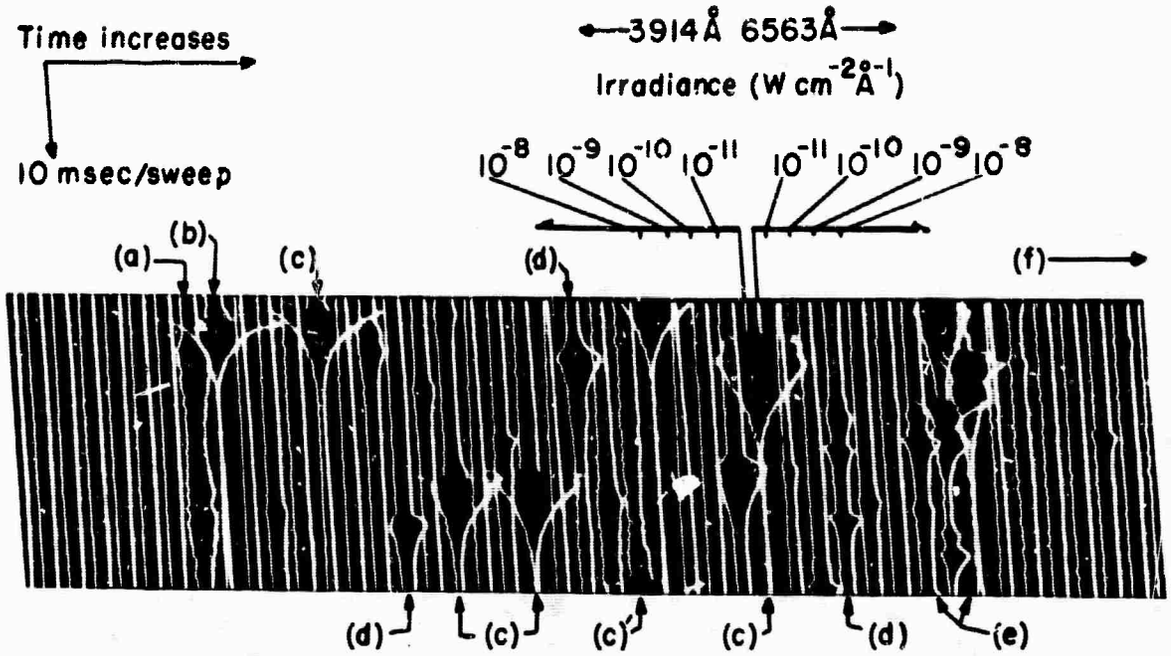

Fig. 4. Typical continuously recorded collimated-photometer incident irradiances from storm 44, flash 182 (9/7/65, 2212 MDT), a ground flash at 27.4-km distance, with two separate vertical channels. This reproduction represents a 400-msec segment of the flash, which lasted about 1 sec. Two simultaneous 10-msec sweeps run from top to bottom of the photograph, then repeat displaced to the right. The callouts are as follows:

(a) A typical stepped-leader signature.
(b) The first return stroke, also the trigger pulse, which occurred 9 msec after the optical onset of the stepped leader.
(c) Subsequent return strokes. Some are preceded within 1 to 2 msec by dart-leader signatures. The one marked (c)′ may be a "first" return stroke associated with the second of the two observed vertical channels.
(d) Intracloud-process pulses, associated with streamers to new charge concentrations within the cloud.
(e) A complicated light pulse, probably produced by a relatively short-lived continuing current.
(f) This record is followed after ~ 150 msec by more pulse activity.

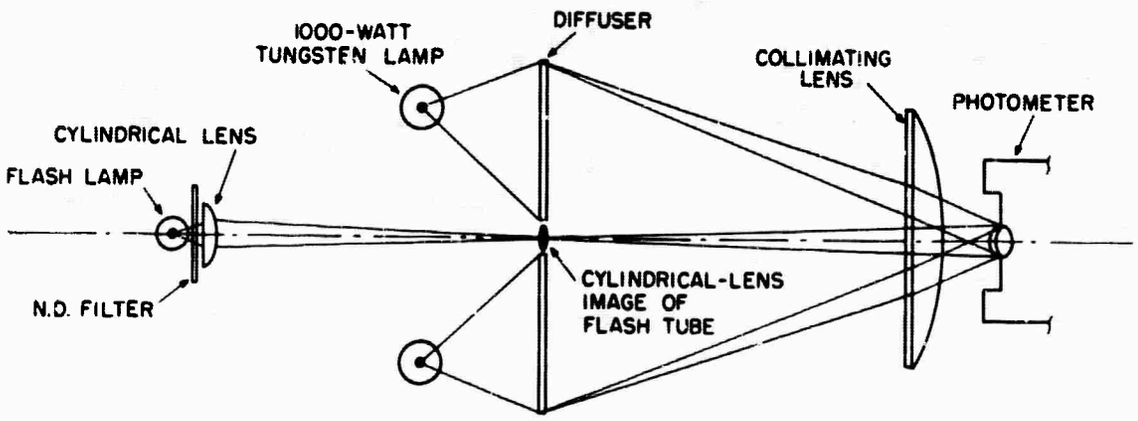

Fig. 5. Calibration apparatus for measurement of fatigue effects. The 1000-W lamps and diffusers produce a uniform background illumination. The cylindrical-lens image of the flash lamp simulates a lightning stroke in the center of the field of view.

view was produced by brightly illiminated diffuse scatterers. A lightning flash was simulated in the center of the field of view by a cylindrical-lens image of the flash-lamp pulse. Curves of relative sensitivity as a function of background current were obtained for all fatigue situations, and a set of such curves is shown in Fig. 6. There was no nonlinearity of output for any of the detectors at any of the voltages or background levels within the range of currents used.

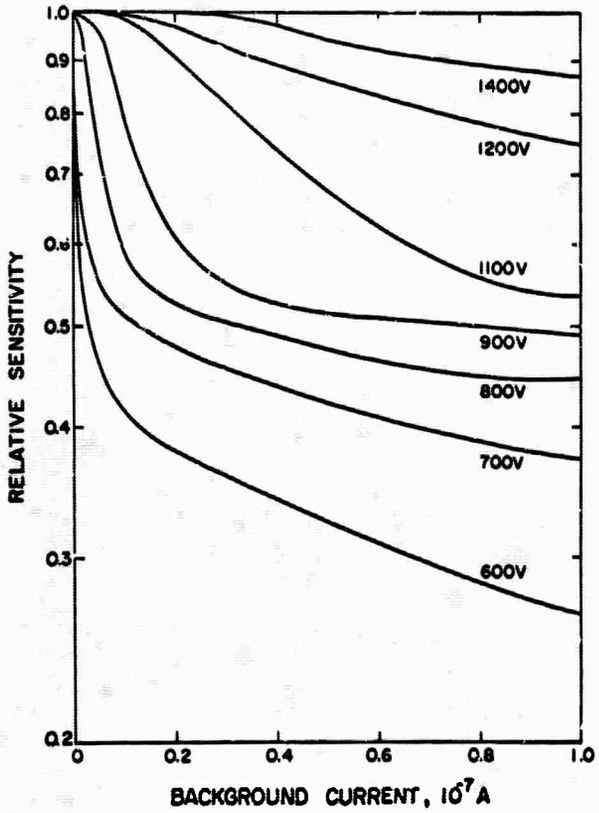

Fig. 6. Changes in sensitivity of 6563-Å collimated photometer produced by background illumination.

The lightning-produced irradiances, $H(\lambda_o)$, quoted in the data reduction were calculated by

$$H(\lambda_o) = I\, S_V(\lambda_o) \quad ,$$

where I is the pulse current measured during the experiment for the photometer channel centered on λ_o. It can be shown[7] that, to a good approximation, $H(\lambda_o)$ is the spectral irradiance, $H(\lambda)$, produced at the detector by lightning, averaged over the interference-filter spectral-passband transmission curve, $T(\lambda,\lambda_o)$; i.e.,

$$H(\lambda_o) = \frac{\int_0^\infty H(\lambda)\, T(\lambda,\lambda_o)\, d\lambda}{\int_0^\infty T(\lambda,\lambda_o)\, d\lambda} \quad .$$

III. DATA REDUCTION

The continuous recordings of the collimated-photometer signals were reduced using photometer and electrical-system calibrations to give incident peak spectral irradiances (W cm^{-2} $Å^{-1}$) for each channel. Peak signals were measured for each of the pulses recorded during lightning flashes selected on the basis of knowledge of distance to the channel and the availability of comparison data from other sensors. The results were (a) spectral irradiance at each photometer entrance pupil for each pulse, and (b) ratios of these values to the spectral irradiance in the 3914-Å channel. Each pulse was identified by a number representing the time (msec) at which the pulse occurred after the coordinated-trigger pulse for that flash. Incident spectral irradiances, calculated from the signals shown in Fig. 4, are given in Table II.

Table II. Incident Peak Spectral Irradiances for Pulses Shown in Fig. 4

Time, msec	Figure 4 Reference	Spectral Irradiance 3914 Å, W cm^{-2} $Å^{-1}$	Spectral Irradiance 6563 Å, W cm^{-2} $Å^{-1}$
-009	(a)	2.0×10^{-12}	7.8×10^{-12}
000	(b)	1.1×10^{-10}	5.7×10^{-10}
040	(c)	1.3×10^{-10}	4.8×10^{-10}
060	-	1.1×10^{-12}	4.9×10^{-12}
077	(d)	2.1×10^{-12}	1.3×10^{-11}
095	(c)	1.6×10^{-11}	1.1×10^{-10}
096	(c)	6.4×10^{-12}	4.3×10^{-11}
125	(c)	2.5×10^{-11}	1.4×10^{-10}
126	(c)	1.2×10^{-11}	8.6×10^{-11}
141	(d)	4.0×10^{-12}	1.9×10^{-11}
168	(c)'	9.7×10^{-11}	6.8×10^{-10}

Results from the collimated photometers for about 1200 pulses from lightning flashes which occurred during four storms have been reduced. Fifty-

eight of the flashes had bright channels to which the distances were determined, either by the photographic triangulation system or, in a few cases, by noting the time between flash and thunder. A few of the flashes were intracloud or ground flashes to which distance was not measured. They were used to increase the sample of data in several areas, as is discussed in detail in Section IV. For the flashes of known distance, in which all discernable pulses were reduced, the average number of pulses was 15; a few flashes consisted of one pulse; and for one, a total of 87 pulses were reduced.

To determine lightning source characteristics, corrections for modifications of the signals produced by distance and by the intervening atmosphere must be made. The distance dependence of the optical signals can be predicted to a first approximation by the inverse-square law: the irradiance, $H(x)$ ($W\ cm^{-2}$), measured at distance x (km) from the source, is related to the source intensity I ($W\ sr^{-1}$), neglecting atmospheric effects, by $I = 10^{10}\ x^2\ H(x)$. The factor of 10^{10} is required to compensate for different units of length in x and $H(x)$. The intensity I is a source characteristic that is independent of source-to-detector distance when corrections for atmospheric effects are made.

Signal modifications are produced in the atmosphere by scattering from constituents that give dispersive (i.e., wavelength-dependent) or nondispersive effects. Dispersive scattering is produced by molecules (Rayleigh scattering) and aerosols (Mie scattering), which for a given detector location are approximately uniformly distributed and cannot change their distributions rapidly. Nondispersive scattering is caused by atmospheric constituents with large particles, viz., rain and fog, which by their nature are highly variable in distribution as a function of space and time.

The effect on a beam of light of wavelength λ (Å) propagating along a path, s, in a scattering medium with an extinction coefficient, $\mu(s,\lambda,t)$ (km^{-1}), that may depend on coordinates, wavelength, and time, can be written as

$$F_\lambda(s) = F_o(\lambda) \exp\left[-\int_s \mu(s,\lambda,t)\, ds\right] ,$$

where: $F_o(\lambda)$ is the flux (W) at wavelength λ which leaves the source in the direction of the detector's entrance pupil; the integral is a line integral over path s (km); and $F_\lambda(s)$ is the flux that reaches the end of the path. For the dispersive component of the atmosphere the extinction coefficient, $\mu_d(\lambda)$, is not a function of space or time, to a good approximation. The flux at distance x can then be written $F_\lambda(x) = F_o(\lambda) \exp[-\mu(\lambda)x]$. The nondispersive component of the atmosphere, however, will have an extinction coefficient, $\mu_{nd}(s,t)$, which, while it does not depend on wavelength, will depend on spatial coordinates and time. Without precise knowledge of this dependence, the line integral given above cannot be evaluated.

This derivation assumes that the scattering is single, and that it is purely a loss mechanism, so that no light is scattered into the detector's entrance pupil. It applies, therefore, to a narrow-field detector pointed directly toward the source. It is also an adequate first-order approximation to the case of the collimated detectors, which had a 50° field of view; modifications which are produced by light scattered into the field of view will be discussed in a later volume.

Effects of the two types of scattering on the collimated-detector lightning data were determined on the basis of the single-scattering, narrow-field-detector model by separate, empirical techniques, as follows.

A. Dispersive Scattering

The average extinction coefficients, $\mu_d(\lambda)$, produced by the dispersive components of the atmosphere were obtained in two steps. It was found that one set of extinction coefficients gave a good fit to all the data, and that therefore the assumption of a homogeneous, time-independent, dispersive atmospheric component was justified.

First, the difference between $\mu_d(\lambda)$ at $\lambda = 3914$ Å and $\lambda = 6563$ Å was obtained empirically by a derivation of the value that gave the best fit to all the data. Values of the ratio of the incident spectral irradiances at 6563 and 3914 Å vs source-to-detector distances, x, were plotted on a semilog

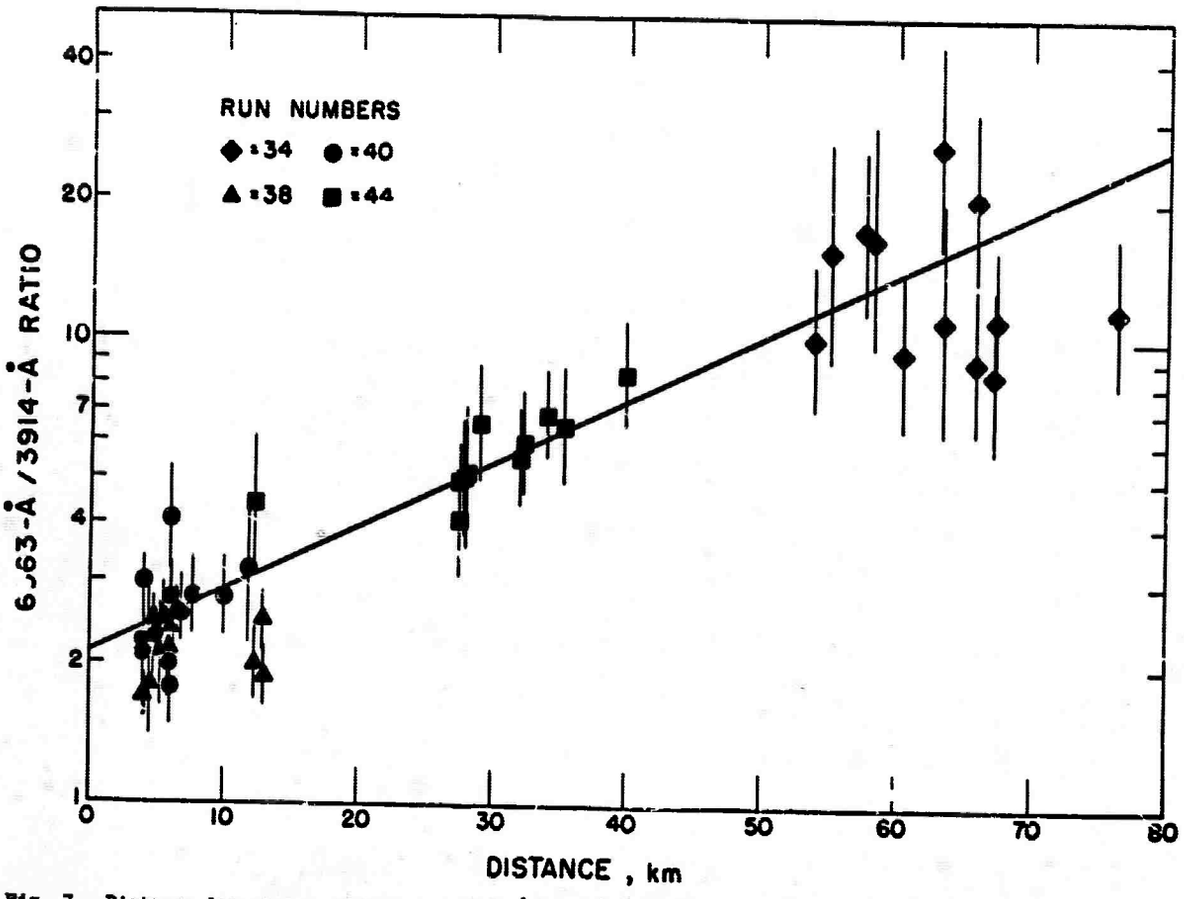

Fig. 7. Distance dependence of incident 6563-Å/3914-Å spectral-irradiance ratio. Each point is the average of all pulse ratios observed for a single flash. The equation of the straight line is RATIO = 2.1 exp(0.031 × DISTANCE), giving an average ratio of 2.1 at the source and a difference of extinction coefficients of 0.031 km^{-1}.

scale, as shown in Fig. 7. The slope of the best straight-line fit to the points then gives $\Delta\mu = \mu_d(3914\ Å) - \mu_d(6563\ Å) = 0.031\ km^{-1}$; the intercept at x = 0 is the average value of the spectral-irradiance ratio which would be measured at the source (given in Section IV).

The second step in the determination of the $\mu_d(\lambda)$ fits the difference given by the first step to tabulated values of typical extinction coefficients of atmospheric constituents. Combined average values of atmospheric molecular and aerosol extinction coefficients are given in the "Handbook of Geophysics and Space Environments,"[8] as a function of wavelength and altitude. An altitude of 4 km produces the difference between extinction coefficients at 3914 and 6563 Å which best agrees with the empirical difference given above. Extinction coefficients $\mu_d(\lambda)$ corresponding to the tabu-

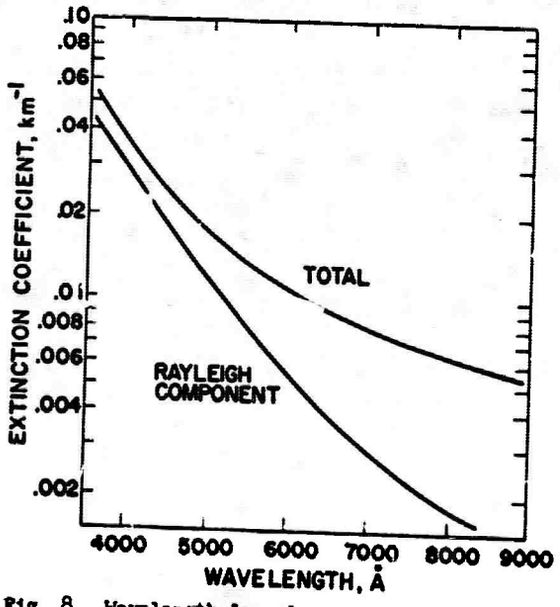

Fig. 8. Wavelength dependence of extinction coefficients for which the difference between values at 3914 and 6563 Å is 0.031 km^{-1}.

lated data for that altitude are plotted vs wavelength in Fig. 8. Shown for comparison is the component produced by Rayleigh scattering alone.

B. Nondispersive Scattering

As mentioned previously, the atmospheric constituents that cause nondispersive scattering are rain and fog, with much more variable effects than the dispersive constituents discussed above. Hence, the assumption of a uniform, time-independent, extinction coefficient, μ_{nd}, which is applicable to all storms is not justified. Corrections could be made for the effects of rain if measurements of the rainfall rate had been made all along each lightning-to-detector path, a clearly impractical approach due to the unpredictable location of lightning channels. Methods exist, but were not used, for probing the atmosphere from one location with optical radar to measure scattering and extinction coefficients on linear paths through that location.[9,10] In lieu of data giving unambiguous values of atmospheric transmission, an empirical method has been used to minimize the dependence of the reduced data on nondispersive atmospheric constituents.

Since the nondispersive scatterers affect all spectral channels equally, only absolute signal magnitudes can be an effective probe of the extinction coefficient. Figure 9 is a plot of the absolute spectral intensity at 3914 Å, corrected for inverse-square law and for dispersive scattering, vs distance to the source. Each point is the average intensity of all pulses of one flash, where the

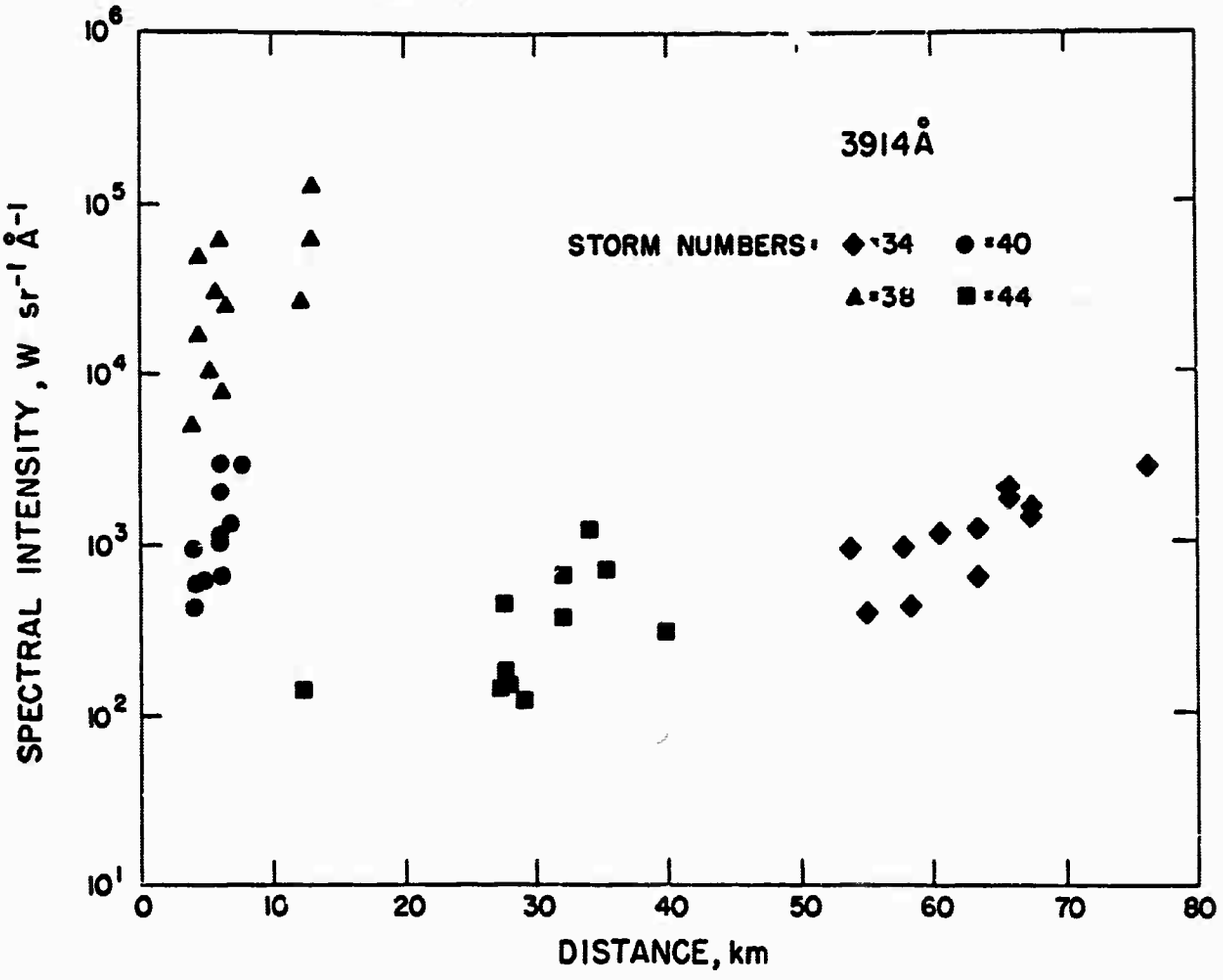

Fig. 9. Distance dependence of 3914-Å spectral intensity. Each point is the average (see text) of all peak spectral intensities for a single flash. The uncorrected effect of nondispersive scattering is obvious.

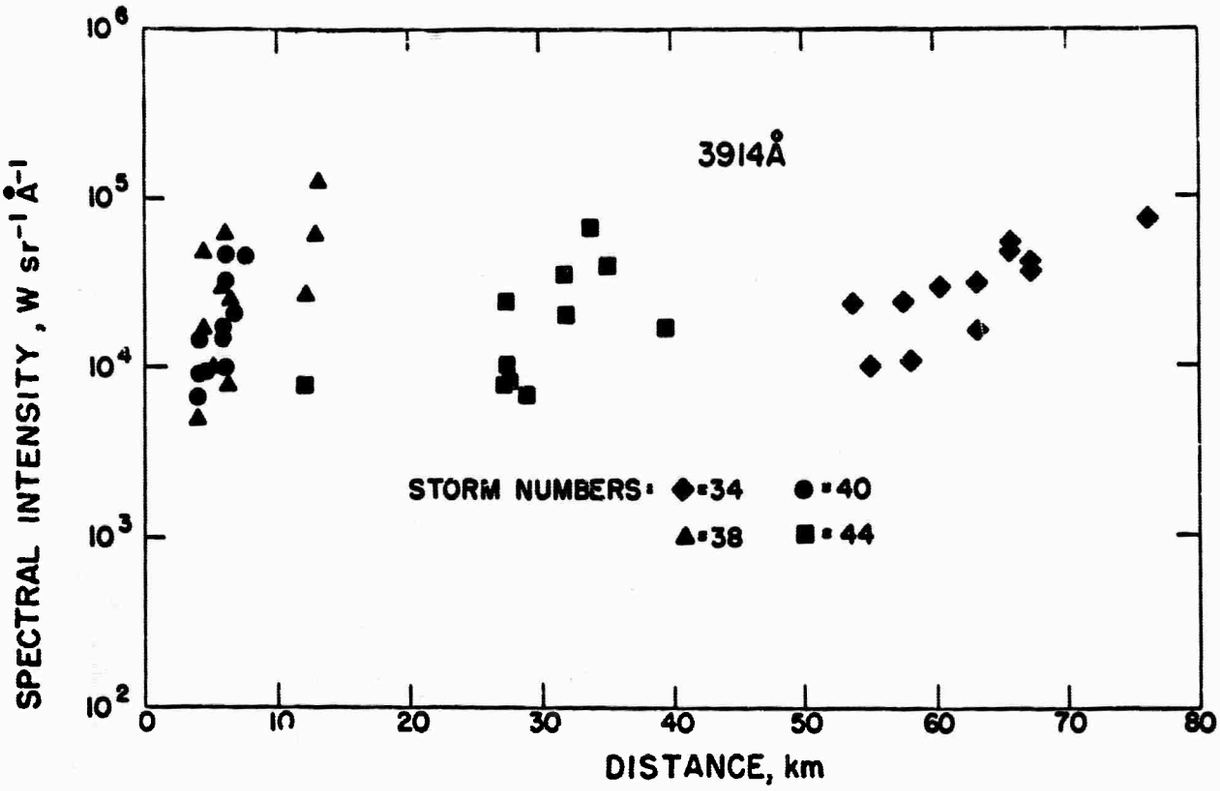

Fig. 10. Distance dependence of 3914-Å spectral intensity. Data are the same as in Fig. 9, but corrected for nondispersive scattering by use of the model discussed in the text. The improvement in consistency is clear.

average was determined from the mean of the logarithms of the intensities. It is clear that points within each storm tend to scatter by a factor of about 10, while comparisons among the storms show differences of more than a factor of 100. Since there is no reason to assume that these storms all had quantitatively different lightning, it is assumed that the differences are produced mainly by atmospheric effects not yet included in the reductions.

A type of correction, suggested by Fig. 9, that serves to bring the data into better agreement, predicates that the atmospheric-transmission correction is the same for all flashes in any given storm. An "extinction factor," by which all intensities must be multiplied, is derived for each storm by requiring that the average intensities for all storms be equal. The following extinction factors were obtained from the data plotted in Fig. 9: storm 34, 27; storm 38, 1.0 (this storm is used as a standard); storm 40, 16; and storm 44, 90. The data corrected by these factors are plotted in Fig. 10, which shows the improvement in data consistency.

This correction accounts only for atmospheric extinction between storm and detector and cannot account for the variations of atmospheric transmission within the storm that produce part of the remaining point scatter in Fig. 10. Furthermore, the data available do not admit of a more refined treatment, since no measurements of extinction coefficients or of data pertaining to them were made. The absolute-intensity distribution function, to be derived from the data corrected for nondispersive scattering on the basis of the one-parameter-per-storm model, therefore represents actual lightning pulse-height variations, without correction for rain and fog within a storm. The false-alarm analysis (Volume IV of this series) will not require that these effects be separated.

To summarize, the data are reduced to source characteristics by corrections for (a) inverse-

square law, to give intensities radiated by the source; (b) dispersive scattering, determined empirically from the incident relative-irradiance data; and (c) nondispersive scattering, determined empirically from the absolute-intensity data.

IV. RESULTS

The optical data have been used to derive source characteristics and their variations. The 3914-Å spectral-intensity distribution function is given, and other results are presented only as spectral intensity relative to 3914 Å, for the following reason. The absolute-intensity distribution function at 3914 Å spans several powers of 10 in intensity, as do those at other wavelengths, owing to the many types of lightning phenomena represented. There is much less pulse-to-pulse variation of the other intensities relative to that at 3914 Å; therefore, variations among absolute-intensity distribution functions would cover but a small fraction of the renge of intensity values of the 3914-Å distribution function. If required, the absolute-intensity distribution function for any of the spectral channels can be derived from the 3914-Å absolute-intensity distribution function and the corresponding relative-intensity distribution function. Furthermore, the false-alarm-rate analysis to be presented in Volume IV of this series requires the functions given here.

A. Spectral Intensity at 3914 Å

Figure 11 is a plot of the distribution function of source spectral intensities at 3914 Å. As discussed in the previous section, this distribution represents that of all pulses produced by a lightning storm, without correction for rain or fog within the storm. Effects of extinction by the atmosphere outside the storm have been removed.

The most probable spectral intensity at 3914 Å is $\sim 10^4$ W sr^{-1} Å^{-1}. Because optical pulses from all types of lightning phenomena, viz. leaders, return strokes, and intracloud processes, were used in the derivation of the distribution, there is a large spread of the spectral intensities, more than a factor of 10 at the half-maximum points.

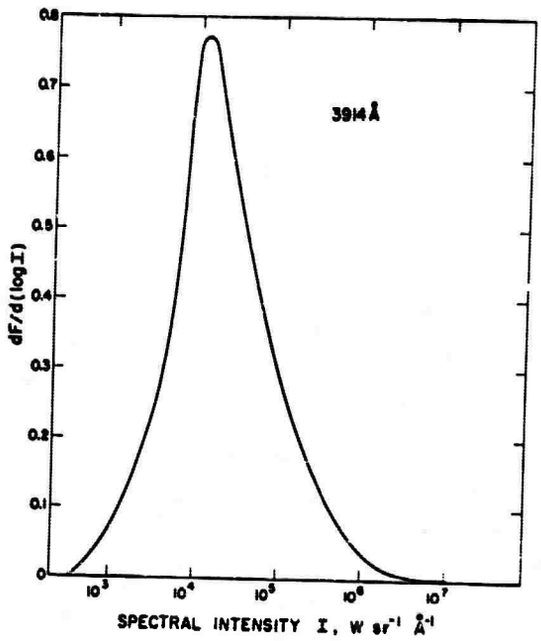

Fig. 11. Distribution function, dF/d(logI), for 3914-Å spectral intensities, I. Logarithms are to base 10. Fraction of pulses with intensities between I_1 and I_2 is $\Delta F = \int_{\log I_1}^{\log I_2} \frac{dF}{d(\log I)}\, d(\log I)$.

B. Spectral Intensities Relative to 3914 Å

Average values of spectral intensities measured at 4140, 6563, 8220, and 8900 Å, relative to 3914 Å, are given in Table III. The numbers of pulses which the averages represent are different because not all detectors were in operation at any one time. The averages given for "all pulses" represent the average pulse a lightning flash produces. Pulses which can be attributed to first return strokes on the basis of the continuous recordings have been isolated in a manner similar to the data reduction of the slitless spectra,[1] and average relative spectral intensities are reported separately in the table.

We found that there were too few data with accurately measured distances in four of the entries listed in Table III (see notes c and i). Three of these entries are for first return strokes, which represent only 5% of all pulses reduced, and the fourth is at 8900 Å where the detector sensitivity was poor. We approximately doubled the sample in these entries by incorporating data for which distances had not been measured, using techniques that

Table III. Relative Spectral Intensities Produced by Lightning

Spectral Feature	Wavelength 3914 Å	4140 Å	6563 Å	8220 Å	8900 Å
Lightning[a]	C[b]	C, NI (6)[b]	C[b], H_α	NI(2)	C
Air fluorescence	N_2^+ 1N (0,0)	$N_2$2P(3,7)	$N_2$1P(7,4)	NI(2)	$N_2$1P(1,0)
All pulses	1	1.2 ± 0.5	2.1 ± 0.8	4.8 ± 2.8	0.8 ± 0.4
Samples/storms	-	409/2	842/4	482/3	89/1[c]
First return strokes	1	1.0 ± 0.2	1.2 ± 0.3	1.5 ± 0.6	0.5 ± 0.2
Samples/storms	-	12/2[d]	26/4	30/3[c]	21/1[c]

Notes: a. C = continuum.

b. Slitless spectra show continuum to be present throughout the visible spectrum, producing the main contribution to signals at 3914 and 4140 Å.[1]

c. To increase data sample, some data have been used for which distances were estimated. See text.

d. To increase data sample, some data from a near storm have been used without correction for distance. Estimated error in 4140-Å/3914-Å ratio is small. See text.

minimized any errors so introduced. First, at 4140 Å, first-return-stroke data from a storm that was localized near (i.e., < 20 km from) the detectors were added without benefit of atmospheric-transmission correction. The average error introduced in the 4140-Å/3914-Å spectral-intensity ratio is < 10%, owing to the small separation in wavelength. Second, for the infrared channels, data were taken from flashes with many pulses, for which distances were estimated empirically, as follows. The average incident spectral-irradiance ratio, 6563 Å/3914 Å, for all pulses in the flash was used as an ordinate in Fig. 7, and the straight line was used to determine the corresponding distance on the abscissa. For a flash with 10 pulses, the probability is 50% that the distance so estimated is within ± 4 km. The average error in the relative infrared-intensity values derived using these estimated distances is ± 20%.

Several conclusions can be obtained or substantiated on the basis of the data in Table III.

(1) The large values of relative spectral intensity at 6563 and 8220 Å are produced by strong excitation, in the average lightning pulse, of the species H_α and NI, respectively. This behavior was also observed in the visible in the slitless spectra.[1]

(2) The small value of the relative 8900-Å spectral intensity shows the absence of a strongly-excited atomic-line or molecular-band feature and only a weak continuum in the infrared.

(3) The first-return-stroke data show a decrease of all red and infrared channels for first return strokes when compared with other pulses. We interpret the decreases as manifestations of two effects observed in the slitless spectra of first return strokes:[1] the decrease of HI and NI features relative to the continuum, and the increase of the blue continuum relative to the red. The 4140-Å/3914-Å spectral-intensity ratio is expected to be relatively unchanged when first return strokes are compared to other pulses, because both channels see primarily continuum and there is little separation in wavelength between them. The 4140-Å data clearly attributable to first return strokes are insufficient to substantiate or invalidate this conclusion.

Histograms of the spectral intensities at 4140, 6563, 8220, and 8900 Å, relative to 3914 Å, are given in Figs. 12 through 15, respectively. Since these histograms are to represent the overall behavior of the various spectral regions in lightning, the data from which they are derived represent all types of lightning phenomena, i.e. all pulses.

For the histograms of the 4140- and 6563-Å relative intensities the most probable ratio agrees well with the average ratio. This signifies that

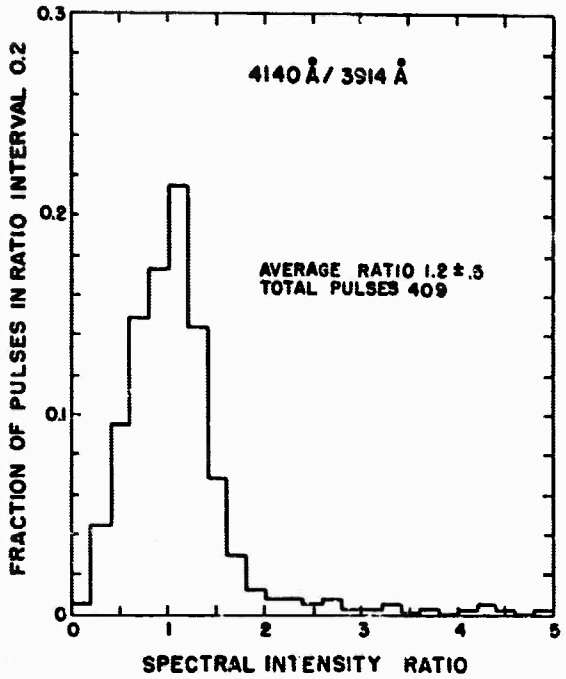

Fig. 12. Histogram of 4140-Å/3914-Å spectral-intensity ratio. No pulse has ratio ≤ 0.1.

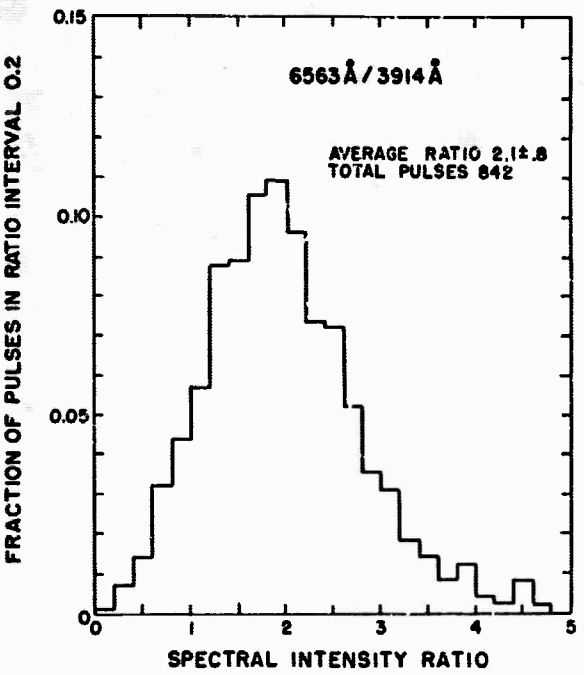

Fig. 13. Histogram of 6563-Å/3914-Å spectral-intensity ratio. No pulse has ratio ≤ 0.1.

the histograms are approximately symmetric about the most probable ratio. This symmetry does not exist in the case of the 8220-Å relative-intensity histogram, which is more heavily weighted by large values

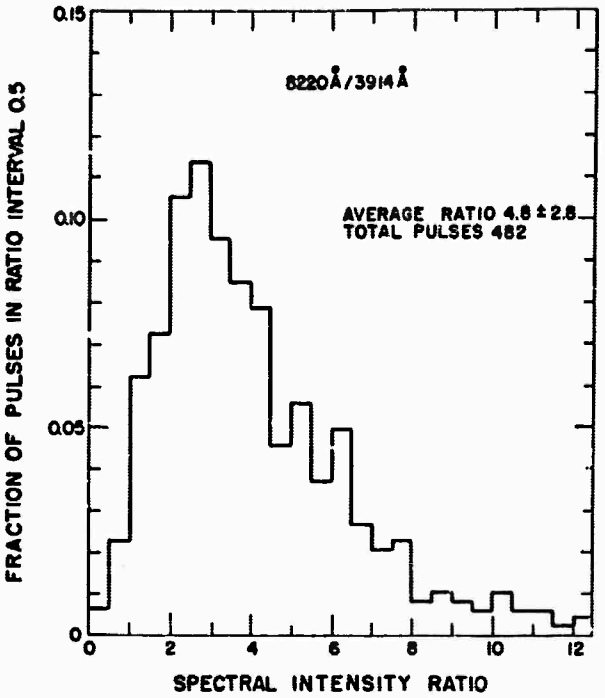

Fig. 14. Histogram of 8220-Å/3914-Å spectral-intensity ratio. Most probable ratio, ~ 3, differs from average ratio, 4.8, owing to relatively large numbers of ratios > 8. See text.

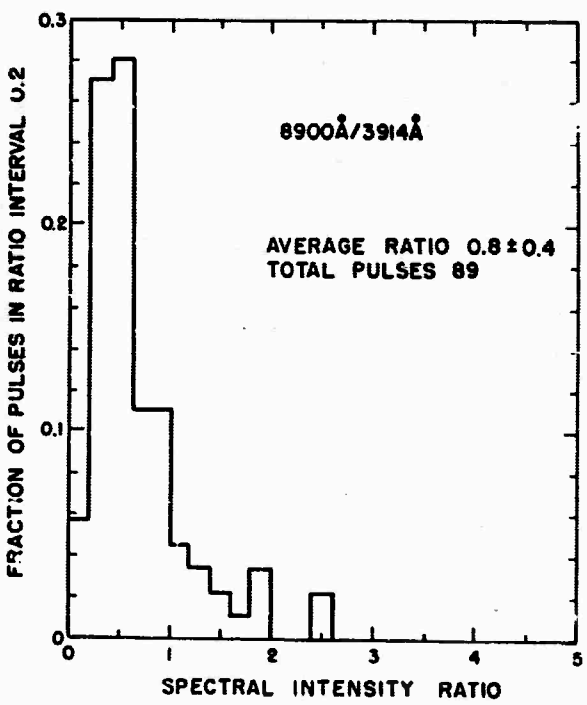

Fig. 15. Histogram of 8900-Å/3914-Å spectral-intensity ratio.

of the intensity ratio. The asymmetry may be real if the large values are produced by enhanced excitation of the NI(2) feature at 8220 Å relative to 3914 Å. We expect large variations of signals in the 8220-Å channel because of the different excitation mechanisms of the NI(2) atomic line for the many types of pulses and the lack of a strong continuum. However, the asymmetry may be the result of an experimental problem caused by the lack of sensitivity of the infrared detectors.

Because it may be of interest in future studies of discrimination against lightning involving detection systems that are sensitive wholly within the infrared, we have compared the 8220- and 8900-Å data with each other. No correction for distance dependence of the 8220-Å/8900-Å ratio was made because of the small predicted difference in extinction coefficients and the relative uncertainty as to how well the atmospheric extinction model can be extended into the infrared. For 89 pulses from one storm, including all phenomena, the average 8220-Å/8900-Å spectral-intensity ratio was 4.8 ± 2.6; for 21 first return strokes it was 3.1 ± 0.9. The difference reflects the lower excitation of the NI(2) (8220-Å) feature in first return strokes relative to the average pulse. A histogram of the all-pulse values is shown in Fig. 16. As in the case of the 8220-Å/3914-Å ratio, the spread of values is large, for the same reasons.

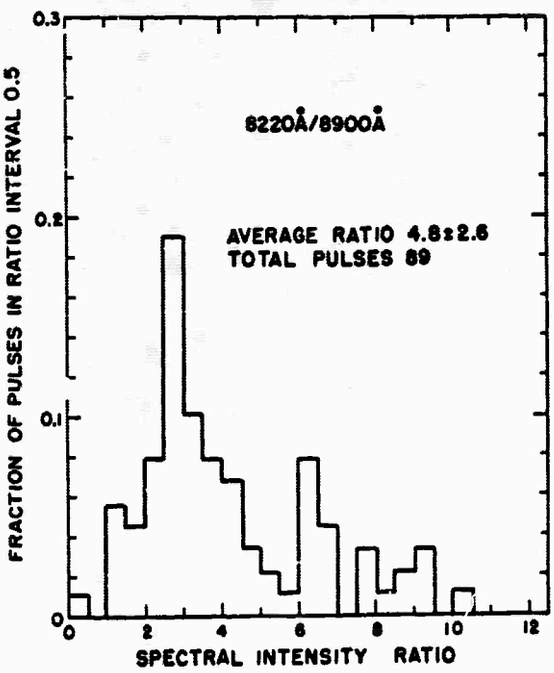

Fig. 16. Histogram of 8220-Å/8900-Å spectral-intensity ratio. Data not corrected for atmospheric extinction. See text.

The distribution functions for the spectral-intensities at 4140, 6563, 8220, and 8900 Å, relative to 3914 Å, given in the histograms of Figs. 12 through 15, are shown in another form in Fig. 17. A similar distribution function for the 8220-Å/8900-Å data is given in Fig. 18. The probability that the

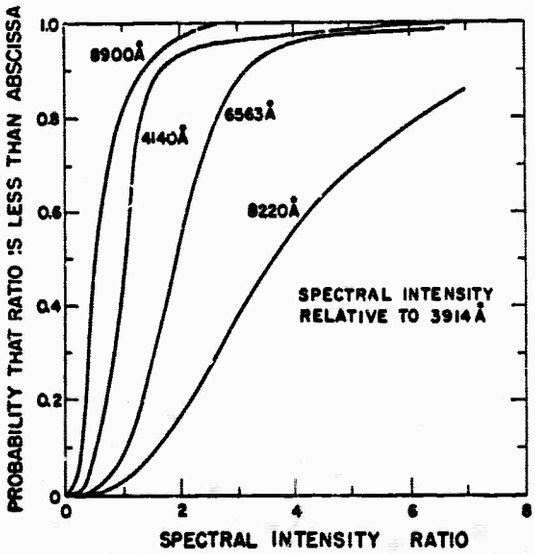

Fig. 17. Distribution functions of spectral intensities at 4140, 6563, 8220, and 8900 Å, relative to 3914 Å.

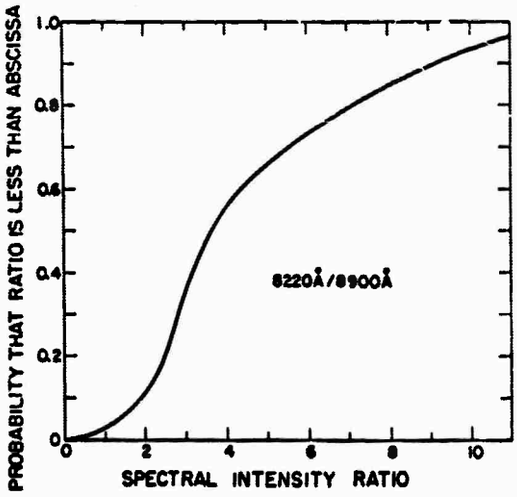

Fig. 18. Distribution function of spectral-intensity ratio 8220 Å/8900 Å.

intensity ratio produced by a given pulse is smaller than some input value in the form of distribution function required by the false-alarm analysis (Volume IV, to be issued).

ACKNOWLEDGMENTS

These measurements were conducted under a program which is part of an ARPA- and AEC-sponsored effort to improve ground-based nuclear-test-detection capabilities and which involved the coordinated efforts of a number of organizations: EG&G, Inc., Boston and Bedford, Massachusetts; Denver Research Institute, Denver, Colorado; Atomic Weapons Research Establishment, Aldermaston, England; and LASL. The cooperation of members of those organizations is gratefully acknowledged. W. Gould performed the photometer calibrations. The photographic triangulation data were read and analyzed by S. Waber and R. Yoakum. Detailed assistance and suggestions by E. W. Bennett and M. Peek have been most helpful.

The coordinated program and subsequent data reduction and analysis have been under the direction of Herman Hoerlin, to whom thanks are due for many helpful suggestions. Thanks are also due to Lt. Col. John Hill and other personnel of the Nuclear Test Detection Division of ARPA for their active interest in the problems.

REFERENCES

1. T. R. Connor, "The 1965 ARPA-AEC Joint Lightning Study at Los Alamos: Volume I. The Lightning Spectrum. Charge Transfer in Lightning. Efficiency of Conversion of Electrical Energy into Visible Radiation," Los Alamos Scientific Laboratory report LA-3754, May 1967.
2. D. R. Westervelt and H. Hoerlin, Proc. IEEE 53, 2067 (1965).
3. R. A. Amato, "Spectral and Temporal Characteristics of Lightning as Measured with a Wide-Angle Detector," EG&G, Inc., report number B-3506, March 1, 1967.
4. E. P. Krider, J. Geophys. Res. 70, 2459 (1965).
5. E. P. Krider, J. Geophys. Res. 71, 3095 (1966).
6. N. Kitagawa and M. Brook, J. Geophys. Res. 65, 1189 (1960).
7. G. E. Barasch, LASL internal document, December 21, 1966.
8. "Handbook of Geophysics and Space Environments," Shea L. Valley, Ed., Air Force Cambridge Research Laboratories, 1965, Chap. 7.
9. G. Fiocco and G. Grams, J. Atmos. Sci. 21, 323 (1964).
10. L. Elterman, Appl. Opt. 5, 1769 (1966).